Photochemical characterization of a new heliorhodopsin from the gram-negative eubacterium *Bellilinea caldifistulae* (BcHeR) and comparison with heliorhodopsin-48C12

Atsushi Shibukawa[1], Keiichi Kojima[1], Yu Nakajima[2], Yosuke Nishimura[2], Susumu Yoshizawa[2,3] & Yuki Sudo[1,*]

[1]Graduate School of Medicine, Dentistry and Pharmaceutical Sciences, Okayama University, Okayama 700-8530, Japan.

[2]Atmosphere and Ocean Research Institute, The University of Tokyo, Chiba 277-8564, Japan.

[3]Department of Natural Environmental Studies, Graduate School of Frontier Sciences, The University of Tokyo, Chiba 277–8563, Japan.

ABSTRACT

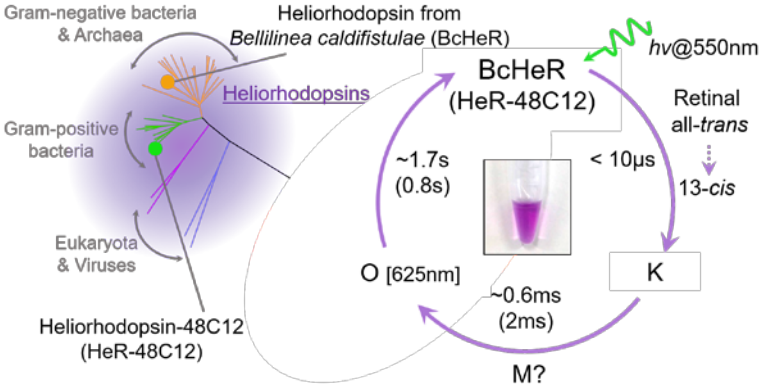

Many microorganisms express rhodopsins, pigmented membrane proteins capable of absorbing sunlight and harnessing that energy for important biological functions such as ATP synthesis and phototaxis. Microbial rhodopsins that have been discovered to date are categorized as type-1 rhodopsins. Interestingly, researchers have very recently unveiled a new microbial rhodopsin family named heliorhodopsins that are phylogenetically distant from type-1 rhodopsins. Among them, only heliorhodopsin-48C12 (HeR-48C12) from a gram-positive eubacterium has been photochemically characterized [Pushkarev *et al.*, 2018, Nature, 558, 595-599]. In this study, we photochemically characterize a purple-colored heliorhodopsin from gram-negative eubacterium *Bellilinea caldifistulae* (BcHeR) as a second example and we identified which properties are or are not conserved between BcHeR and HeR-48C12. A series of photochemical measurements revealed several conserved properties between them, including a visible absorption spectrum with a maximum at around 550 nm, the lack of ion-transport activity, and the existence of a second-order O-like intermediate during the photocycle that may activate an unidentified biological function. In contrast, as a property that is not conserved, although HeR-48C12 shows the light-adaptation state of retinal, BcHeR showed the same retinal configuration both in dark- and in light-adapted conditions. These comparisons of photochemical properties between BcHeR and HeR-48C12 are an important first step toward understanding the nature and functional role of heliorhodopsins.

INTRODUCTION

Many microorganisms are now well-known to absorb sunlight via microbial rhodopsins with a retinal chromophore (vitamin A aldehyde), whose energy is harnessed for important biological processes such as ATP synthesis and phototaxis.[1] Since the first recognition of bacteriorhodopsin (BR) in *Halobacterium salinarum* in 1971,[2] the expedition towards further identification and characterization of microbial rhodopsins has started. Indeed, a large variety of microbial rhodopsins have been discovered and shown to exhibit various light-triggered functions, including acting as ion-pumps,[3–6] ion-channels,[7,8] and light-sensors.[9–12] For instance, the light irradiation induces ion-pump rhodopsins such as BR[2] and proteorhodopsin (PR) [4] to pump a proton against its concentration gradient across cell membranes, while ion-channel rhodopsins open molecular gates through which many cations or anions can pass across the membrane,[7,8] resulting in large photocurrents. Such an attractive characteristic of ion-channel rhodopsins has been extensively exploited in optogenetics fields to depolarize or hyperpolarize cells in a controllable manner.[13]

One approach to explore microbial rhodopsins is based on homology searches by screening whole genomes from microorganisms[14] or metagenomes from environmental samples.[15] Phenotypic screenings with *Escherichia coli* (*E. coli*) cells expressing heterologously putative rhodopsin genes have also been attempted in the presence of exogenous all-*trans* retinal. One such study identified *E. coli* cells displaying an orange to red phenotype[16] and another study was based on light-induced pH changes of solutions containing *E. coli* cells.[17] In those studies, diverse marine microbial rhodopsins were successfully detected based on the color of *E. coli* cells heterologously expressing the cloned DNA. Importantly, unlike homology searches, these methods allow the discovery of rhodopsins that have not been identified so far and are genetically distant from known microbial rhodopsins. Indeed, in 2018, based on the pigmentation of *E. coli* cells, a fosmid library from a fresh water habitat was screened and a previously uncharacterized rhodopsin family named heliorhodopsins was revealed.[18] Such heliorhodopsins shape a genetically distant group from the known microbial rhodopsins (type-1 rhodopsins) but they still contain seven transmembrane helices and a lysine residue in the seventh helix that is conserved in type-1 rhodopsins (Figure 1). Among them, only heliorhodopsin 48C12 (HeR-48C12) from a gram-positive actinobacterium has been fully characterized[18].

Independently from the above study, we screened twenty-four previously unknown rhodopsin-like proteins identified from the database (https://www.ncbi.nlm.nih.gov) and half of them (twelve) were confirmed to be pigmented when expressed in *E. coli* cells. Later, it turned out that they are phylogenetically classified into the heliorhodopsin family. In this study, we photochemically characterized one such heliorhodopsin as a second example, a purple-colored heliorhodopsin from gram-negative eubacterium *Bellilinea caldifistulae* (BcHeR), and we reveal conserved photochemical properties between BcHeR and HeR-48C12. From a series of

photochemical measurements, as conserved properties, we show that BcHeR presents an absorption maximum of 550 nm, the lack of ion-transport activity, and a second-scale long O-like intermediate in the photocycle. On the other hand, as a property that is not conserved, we show that the retinal adaptation state is absent in BcHeR while HeR-48C12[18] has been reported to show a light-adaptation state.

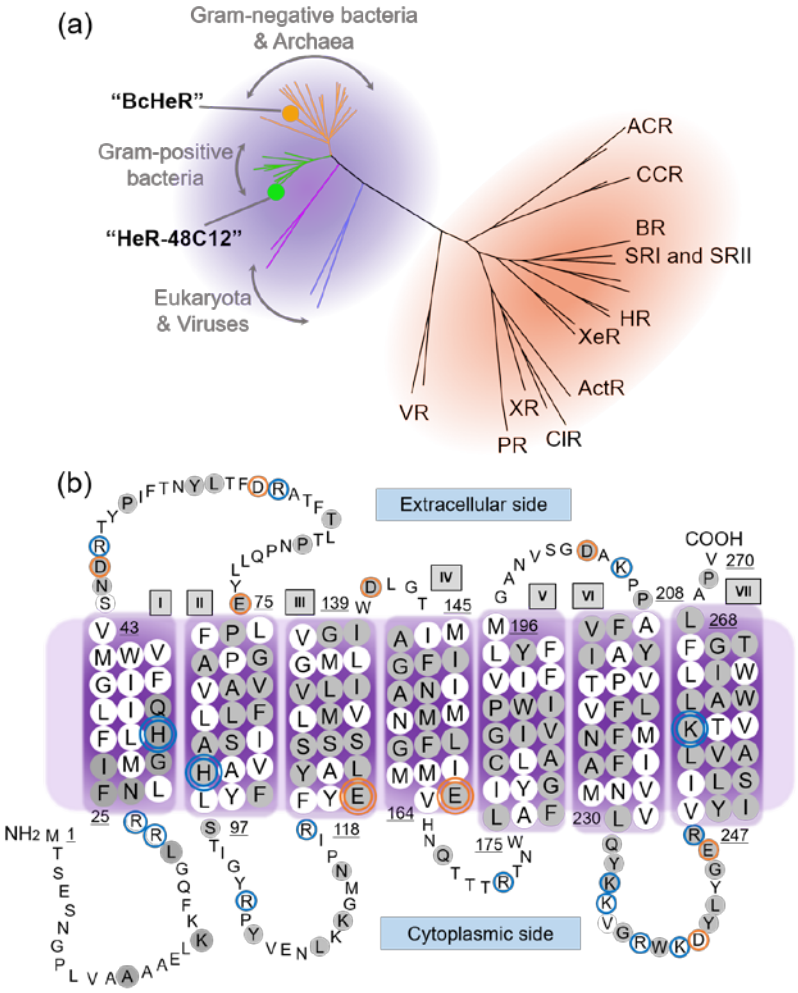

Figure 1. *B. caldifistulae* heliorhodopsin (BcHeR). (a) Phylogenetic tree separating heliorhodopsins and type-1 microbial rhodopsins into two distinct groups. The heliorhodopsin family is divided into an orange clade of 'gram-negative bacteria and archaea', a green clade of 'gram-positive bacteria' and purple and blue clades of 'eukaryota and viruses', respectively. As expected, BcHeR and HeR-48C12 were assigned into gram-negative bacteria and gram-positive bacteria clades, respectively. ACR, anion channelrhodopsin; CCR, cation channelrhodopsin; BR, bacteriorhodopsin; SRI and SRII, sensory rhodopsin I and II; HR, halorhodopsin; XeR, xenorhodopsin; ActR, actinorhodopsin; ClR, chloride pumping rhodopsin; XR, xanthorhodopsin; PR, proteorhodopsin; VR, viral rhodopsin. See Table S1 for accession codes of all rhodopsins used in the analysis. (b) Predicted secondary structure of BcHeR. Residues (double-)circled in blue or orange denote positively or negatively charged amino acids (inside putative transmembrane helices), respectively. Filled gray circles denote amino acids shared by BcHeR and HeR-48C12. Roman numbers ('I' to 'VII') indicate helix numbers.

MATERIALS AND METHODS

Gene construction of BcHeR.

The DNA fragment encoding BcHeR (accession code: KPL76735.1) present in *B. caldifistulae* GOMI-1^T was chemically synthesized by Eurofins Genomics (Japan) with codon optimization for *E. coli* cells. This gene fragment was inserted into the NdeI and XhoI restriction enzyme sites of the pET21a vector (Novagen, USA); the plasmid also encoded a hexahistidine sequence at the C-terminus of BcHeR.

Expression of BcHeR in *E. coli* membranes. The *E. coli* BL21(DE3) strain containing the histidine-tagged BcHeR plasmid was incubated at 37 °C in standard LB medium (10 g/L tryptone, 5 g/L yeast extract and 10 g/L NaCl) in the presence of 50 μg/mL ampicillin until the absorbance at 660 nm reached an optical density (OD) of around 1.3. Protein expression was then induced for 4 h at 37 °C by adding isopropyl β-D-1-thiogalactopyranoside (IPTG) at a 1 mM final concentration and all-*trans* retinal at a 10 μM final concentration as a chromophore. *E. coli* cells expressing recombinant proteins were washed twice with a buffer (50 mM Tris-HCl at a pH of 7.0 and 300 mM NaCl) and harvested by centrifugation (5,530×g, 15 min, 4 °C).

Purification of BcHeR. The BcHeR expressing *E. coli* cells were suspended in buffer (50 mM Tris-HCl at a pH of 7.0 and 300 mM NaCl) and were disrupted in ice-cold water with an ultrasonic disruptor (UD-211, TOMY) in which the rate of oscillating time per sec was 50 % and the duration was 20 min. The membrane fractions were collected by ultracentrifugation (178,200×g, 60 min, 4 °C) and were solubilized with 1.5 % (w/v) detergent n-dodecyl-β-D-maltoside (DDM, Chemical Dojin) in the buffer. The solubilized proteins were again ultracentrifuged (178,200×g, 60 min, 4 °C) and the supernatant was applied to a Ni^{2+} affinity column (HisTrap ™ FF, 5 ml, GE Healthcare). The proteins loaded on the resin were purified with a linear gradient of imidazole over a concentration range from 0 M to 1 M and the purified proteins were mostly collected in the range from 140 mM to 240 mM imidazole. The purified proteins were concentrated and their buffer was exchanged by centrifugation (5,530×g, 15 min, 4 °C) with an Amicon Ultra filter (30000 Mw cut-off; Millipore). For all experiments except the ion transport and pH titration measurements, the buffer used contained 50 mM Tris-HCl (pH = 7.0), 300 mM NaCl and 0.05 % DDM.

Sample preparation of archaerhodopsin-3. Gene construction, expression in *E. coli* membranes, and purification of archaerhodopsin-3 (AR3) were conducted as described previously.[19] AR3 was used as a control in the measurements of UV-Visible spectra, high-performance liquid chromatography (HPLC), and ion-transport assay.

Phylogenetic tree. To visualize the phylogenetic position of BcHeR among heliorhodopsins and type-1 rhodopsins, we constructed a phylogenetic tree including representative proteins from heliorhodopsins and type-1 rhodopsins used in a previous work.[18] Evolutionary analyses were

conducted using the free MEGA6 software;[20] multiple amino acid sequences were aligned using MUSCLE,[21] the evolutionary distances were estimated by using the JTT matrix-based method,[22] and the Neighbor-Joining tree was constructed.[23] The constructed phylogenetic tree was edited by the free FigTree v1.4.3 software (http://tree.bio.ed.ac.uk/software/figtree/). Amino acid sequences and accession numbers for all rhodopsins used in this analysis are summarized in Table S1.

UV-Visible spectroscopy. UV-Visible absorption spectra were obtained using a spectrometer (UV-1850, Shimadzu). For light-illuminated condition, the purified sample was illuminated with 10 mW/cm^2, 550 nm light for 3 min before the measurement. The illuminated light was generated from a Xenon lamp (MAX-303, Asahi Spectra) combined with a bandpass filter of 550 ± 10 nm. For dark condition, the sample was stored for more than 2 days in the dark at 4 °C before the measurement. The concentration of BcHeR protein at the time of measurement was adjusted to be around 40 µM based on a molar absorbance coefficient ε of reported rhodopsins with all-*trans* retinal (ε = 50000 (L/mol/cm)).

HPLC. Retinal configuration was determined using an HPLC system consisting of a solvent delivery unit (LC-20AT, Shimadzu, Japan), a silica column (6.0×150 mm; YMC-Pack SIL, YMC) and an UV/visible detector (SPD-20A, Shimadzu). The composition of the solvent was 12 % (v/v) ethyl acetate, 0.12 % (v/v) ethanol and 88 % (v/v) hexane (HPLC grade, Wako Pure Chemical Industries, Japan). The BcHeR was denaturized by the addition of methanol to the BcHeR solution to a concentration of 75 % (v/v) and following addition of 1 M hydroxylamine to a concentration of 80 mM. The resulting retinal oximes were extracted by mixing with hexane. . The concentration of BcHeR at the time of measurement was adjusted to 20 µM. Each peak of measured HPLC patterns was assigned to each retinal isomer by comparison with the HPLC patterns from authentic all-*trans* and 13-*cis* retinal oximes, as described previously.[24] The composition of retinal isomers was calculated by integrating the areas of the peaks monitored at 360 nm. For light-illuminated condition, the sample was irradiated with 10 mW/cm^2, 550 nm light for 3 min before the measurement. For dark condition, the sample was kept for more than 2 days in the dark at 4 °C before the measurement.

Ion transport measurements. The *E. coli* cells were washed three times with unbuffered 300 mM NaCl solution and were then resuspended in the same solution. For ion transport activity assay, the cell suspension was illuminated with 10 mW/cm^2, 550 nm light. The light-induced pH changes were measured with a pH electrode (9615S-10D, HORIBA, Japan). Measurements were repeated under the same conditions with the addition of carbonyl cyanide *m*-chlorophenyl hydrazone (CCCP) at a 30 µM final concentration.

pH titration. The sample was suspended in a 6-mix buffer (0.89 mM citric acid, 0.89 mM MES, 1.1 mM TES, 0.78 mM TAPS, 1.1 mM CHES and 0.33 mM CAPS) with 300 mM NaCl and

0.05 % DDM. The final concentration of BcHeR protein was 20 µM. The sample pH was adjusted to the desired values by adding 100 mM HCl or NaOH. The absorption spectrum of the sample at each pH was measured with a UV-visible spectrometer (UV-2450, Shimadzu).

Laser-flash photolysis. The BcHeR protein was suspended in the buffer at a final concentration of 20 µM. The sample was excited by a 550 nm flash light with a nano-second pulsed Nd;YAG laser (Surelite I-10, Continuum, USA) and an optical parametric oscillator (Surelite OPO Plus, Continuum, USA), as detailed previously.[6] In synchronization with the flash light, the sample was illuminated with a probe light, monochromated output of a halogen lump through a monochromator (CT-10, Jasco). For recording time-resolved absorption changes at specific wavelengths, the intensity of the probe light passing through the sample before and after the excitation was monitored by a side-on photomultiplier tube (H8249-102, Hamamatsu Photonics, Japan). To improve the signal-to-noise ratio, measurements of the absorption changes were repeated more than 10 times and were then averaged. Signals within the first 10 µs after the excitation were ignored due to the presence of the scattered flash light. The temperature of the sample in a plastic cuvette was kept at 25 °C using a thermostat. Time evolutions of the absorption spectra at each wavelength were fitted using two exponential equations as follows;

$$\Delta OD(t) = a * exp\left(-\frac{t}{\tau_1}\right) + b * exp\left(-\frac{t}{\tau_2}\right), \quad (1)$$

where t is the elapsed time from the onset of the measurement t_0, ΔOD is the difference in absorbance at $t0$ and t, a and b are coefficients representing the amplitudes of each exponential curve, and τ_1 and τ_2 are time constants.

RESULTS AND DISCUSSION

Heliorhodopsin from the gram-negative eubacterium *B. caldifistulae* (BcHeR).

As mentioned above, we found twelve new rhodopsin genes based on the pigmentation of *E. coli* cells and later they were found to belong to the heliorhodopsin family. In this study, we introduce and characterize one of those heliorhodopsins, a heliorhodopsin from *B. caldifistulae* (BcHeR) (Figure 1), to understand which properties are conserved among the heliorhodopsin family. *B. caldifistulae* itself was isolated from a thermophilic digester sludge and it belongs to the class *Anaerolineae* of the bacterial phylum *Chloroflexi*. Members of the class *Anaerolineae* are known to inhabit high-temperature (45-65 °C), anaerobic and low irradiance environments.[25] In fact, the closest relative (named *Bellilinea* sp. OUT-31) in the class *Anaerolineae* was identified from the undermat of the Mushroom Spring within Yellowstone National Park.[26] It is interesting to note that, despite their environment with low irradiance, both organisms, of *B. caldifistulae* and *Bellilinea* sp. OUT-31, possess hypothetical light-absorbing proteins in their membranes. From the classification of all open reading frames encoding rhodopsins from the *Tara* oceans and from fresh water metagenomes, Flores-Uribe *et al*. revealed that heliorhodopsins are only present in

monoderms (gram-positive bacteria) having an inner membrane, not in diderms (gram-negative bacteria) having inner and outer membranes.[27] This finding supported the hypothesis that heliorhodopsins expressed in the inner membrane of monoderms transport amphiphilic molecules and that the presence of the outer membrane in gram-negative bacteria hampers such molecule transport. Although *B. caldifistulae* is classified into the gram-negative bacteria family that is usually thought to have two (inner and outer) membranes, members of the phylum *Chloroflexi* to which *B. caldifistulae* belongs are exceptional gram-negative bacteria possessing only an inner membrane.[28] Thus, the presence of heliorhodopsin in *B. caldifistulae* is still consistent with the claim that heliorhodopsins function as a transporter of amphiphilic molecules.[27] The investigation of the presence of BcHeR in the inner membrane of the native organism *B. caldifistulae* would be necessary in future. It should be also noted that the genome of the strain *B. caldifistulae* contains not only the heliorhodopsin (BcHeR) but also a putative sodium ion-pumping rhodopsin (Accession Code: GAP09179) while the genes encoding transducer-like proteins such as Htr-I and II for sensory rhodopsins are absent in that genome. In addition, *B. caldifistulae* conserves putative genes involving flagellar motility in the genome, however the motility and flagella has not been confirmed[25].

To visualize the phylogenetic position of BcHeR among the heliorhodopsins and the known type-1 rhodopsins, we constructed the phylogenetic tree shown in Figure 1(a). The heliorhodopsins including BcHeR (filled purple) clearly formed a group distinct from type-1 rhodopsins (filled orange). Among the heliorhodopsin family, each colored clade could be assigned into a different organism species (orange clade; gram-negative bacteria and archaea, green clade; gram-positive bacteria, purple and blue clades; eukaryotes and viruses). BcHeR was correctly located on the clade of gram-negative bacteria while HeR-48C12 was distantly located on the clade of gram-positive bacteria. The identity and similarity of amino acid sequences between BcHeR and HeR-48C12 were 44 % and 62 %, respectively (see Table S1 for the identity and similarity among all heliorhodopsins compared with BcHeR).

Figure 1(b) shows the secondary structure of BcHeR predicted by the free Philius software,[29] in which amino acid residues commonly conserved between BcHeR and HeR-48C12 are marked by filled gray, while positively or negatively charged residues (inside helices) are marked by blue and orange (double-) circles, respectively. As in type-1 rhodopsins,[1,30,31] BcHeR contains seven transmembrane helices and a lysine residue (K253) that forms a protonated Schiff base with the retinal chromophore in the seventh helix (see Figure 4(a) and Figure S1). BcHeR was predicted to have its N terminus in the cytoplasm, which is opposite to type-1 rhodopsins that have their C terminus in the cytoplasm. This inverted membrane topology has been experimentally validated for HeR-48C12[18] as a recombinant protein in *E. coli* cells. However, it would be more meaningful to validate that topology using the protein expressed in a ‘native

organism'. Since it is known that the native organism '*B. caldifistulae*' for BcHeR can be cultured,[25] we will characterize the membrane topology of BcHeR expressed in the native organism in the future. Further, from the mutation analysis of K241 and E107 in HeR-48C12[18] and the amino acid alignment between HeR-48C12 and BcHeR (Figure S1), K253 and E118 in BcHeR can be predicted to be retinal-binding residue via the protonated Schiff base and its counterion, respectively. By performing the mutational analysis of the residue E118, we will experimentally determine the residue of the counterion in future work.

Functional and photochemical properties.

Many microbial rhodopsins show light-driven ion-transport activity, which is one of their representative functions. We measured whether BcHeR also shows ion transport activity when expressed in *E. coli* cells. Archaerhodopsin-3 (AR3), used as a positive control, and BcHeR were expressed in *E. coli* cells and were suspended in unbuffered 300 mM NaCl solution. Carbonyl cyanide *m*-chlorophenyl hydrazone (CCCP) at a 30 μM final concentration was used as a protonophore. In general, ion transport activities of rhodopsins in *E. coli* cells are always accompanied by proton transport upon illumination. In the presence of CCCP as the protonophore, such proton transport is abolished for proton-transporting rhodopsin[32] or is enhanced for other ion-transporting ones.[5]

As seen in the insert of Figure 2, *E. coli* cells expressing BcHeR have a purple color due to their absorption at around 550 nm, while AR3 also absorbs 550 nm light maximally.[19] Therefore, these samples were excited at 550 nm light. The control AR3 has been proved to function as an outward proton-pump[33] and this was confirmed in this experiment as well as shown in Figure 2. The light illumination caused a significant pH decrease because AR3 pumps protons outwardly across the membrane (solid orange), while the addition of CCCP elicited no pH change because the proton gradient produced by AR3 is rapidly dissipated due to the added CCCP (dotted orange). In contrast, regardless of the presence or absence of CCCP, BcHeR produced no detectable pH change upon illumination (solid and dotted blues), meaning that BcHeR did not transport any ions (Na^+, Cl^- and H^+) contained in the solution and does not function as an ion pump or channel. This could be observed as well in the case of HeR-48C12 and the absence of ion transport activity for both BcHeR and HeR-48C12 may indicate that the heliorhodopsin family has other functions such as a light-sensor or the light-induced transport of molecules such as glycopeptides or amphiphilic molecules as proposed in previous studies.[18,27,34]

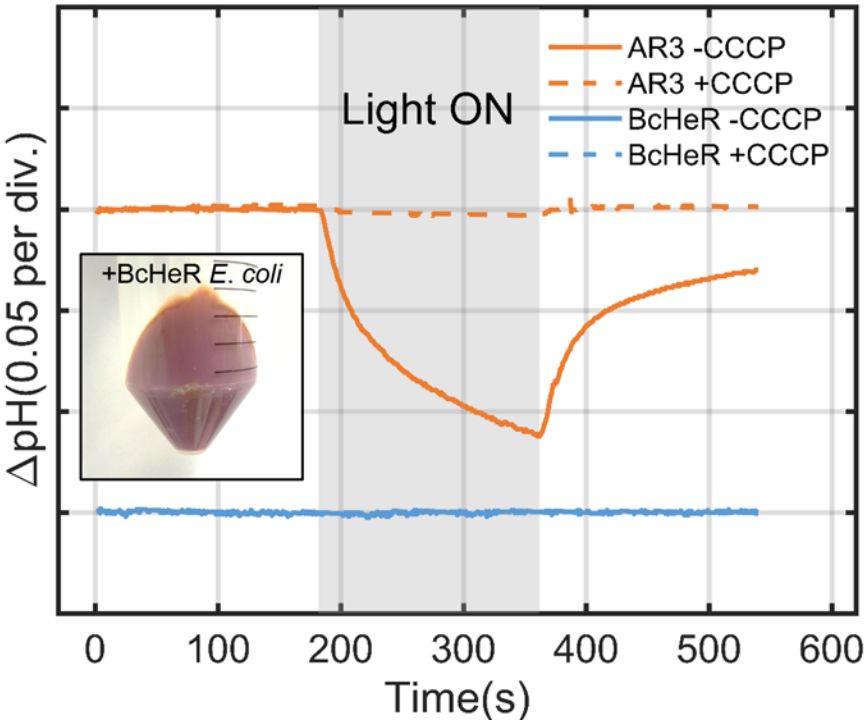

Figure 2. Ion transport measurement. The light-induced pH changes of *E. coli* cell suspensions were observed in the absence (solid line) and in the presence (dotted line) of CCCP. For ion transport activity assays, the cell suspensions were illuminated at 550 nm, 10 mW/cm^2 for 3 min in unbuffered 300 mM NaCl solution. While AR3, used as a control, showed a pH decrease in the absence of CCCP (outward proton-pumping activity), BcHeR showed no pH change regardless of the presence or absence of CCCP (no ion transport activity). The insert shows collected *E. coli* cells expressing BcHeR. Initial pH values for AR3 and BcHeR were 6.49 and 6.45, respectively.

We next characterized the absorption spectra and retinal configuration of purified BcHeR in dark- and in light-illuminated conditions. Many microbial rhodopsins and even HeR-48C12 present not only a light-adapted state[18] but also a dark-adapted state.[35] In the dark-adapted state, a significant portion of all-*trans* retinal transforms into the 13-*cis* form and this retinal structural change blue-shifts the absorption spectrum.[36] AR3 is one such example possessing a dark-adapted state. As seen in Figures 3(a) and 3(b), light illumination of AR3 red-shifted the absorption spectrum by 8 nm (from 552 nm to 560 nm) and caused a predominantly all-*trans* retinal configuration (from 48 % to 89 % in the proportion of all-*trans* form), which correlated well with a previous study (the proportion of all-*trans* form; 53 % in the dark-adapted state, 90 % in the light-adapted state).[19] In contrast, BcHeR showed no such difference; under both dark- and light-illuminated conditions the absorption spectrum showed a maximum at around 550 nm and the retinal takes approximately 88 % all-*trans* form in the configuration (Table 1). The absorption maximum at 550 nm is almost identical to that of HeR-48C12 (Table 1) and causes BcHeR to have a purple color as seen in the insert of Figure 3(a). Since the purple-colored rhodopsin absorbs green light (around 550 nm) maximally, the heliorhodopsin family may be categorized as green-

absorbing rhodopsins. The results shown in Figures 3(a) and 3(b) also revealed that the retinal adaptation state in dark- or in light-adapted conditions is absent in BcHeR, which is clearly a property that are not conserved in comparison with HeR-48C12. This characteristic difference between BcHeR and HeR-48C12 indicates that the presence/absence of the retinal-adaption state may not be important for the function of heliorhodopsins.

In many microbial rhodopsins, the all-*trans* form of the retinal is an active state while the 13-*cis* form is an inactive state for producing their biological functions. For example, for proton-pumping *Rubricoccus marinus* xenorhodopsin,[6] the portion of the 13-*cis* form as the inactive state increases under a high-irradiance environment, probably in order to adaptively reduce the efficiency of the pumping activity. The same senario could be applied to HeR-48C12. This heliorhodopsin was found in Lake Kinneret of Israel which has a 'high-irradiance in daytime' and a 'low-irradiance in night'.[18] Due to such an environment, HeR-48C12 may have gained the ability to switch its retinal configuration to adaptively adjust its biological function depending on the strength of the light irradiance. In contrast, BcHeR was isolated from a thermophilic digester sludge in which the light irradiance is always extremely low regardless of whether it is daytime or night. Therefore, rhodopsins such as BcHeR that live under a habitually low-irradiance environment may evolutionally lose the switching ability of their retinal configuration.

It has been difficult so far to determine the biological function of BcHeR. One effective way to predict the function or substrate ion(s) for BcHeR is to measure dose-dependent maximum absorbance changes with different ions. Indeed, from the observation of absorbance spectral changes, the substrate ion has been successfully confirmed for microbial rhodopsins such as

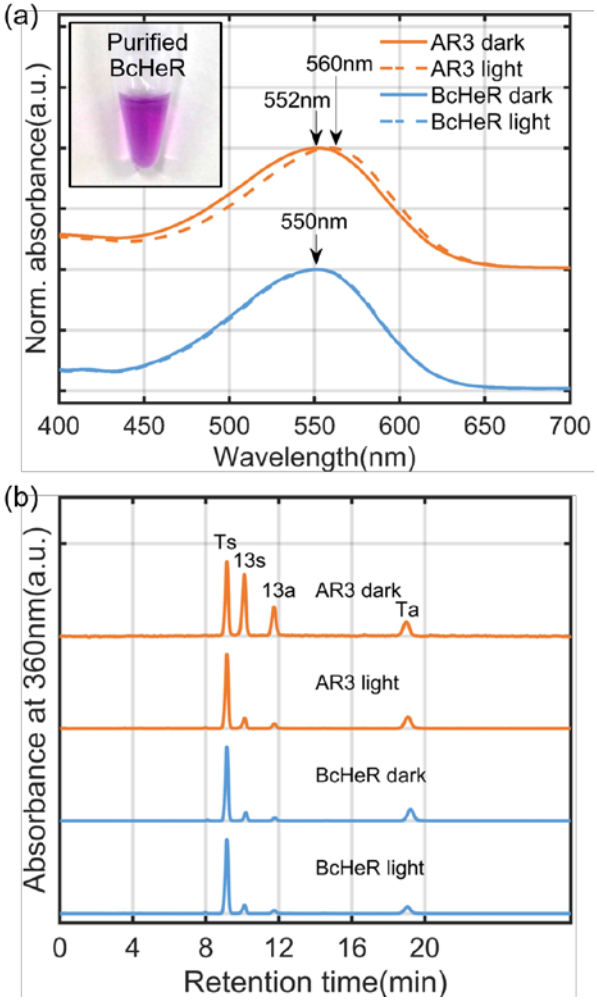

Figure 3. Visible absorption spectra and retinal configuration of purified BcHeR. As a representative type-1 rhodopsin, AR3 was used as a positive control. (a) Absorption spectra of AR3 and BcHeR in dark- and in light-adapted conditions (solid and dotted lines). An absorption peak of BcHeR was detected at around 550 nm and almost no spectral change was observed in dark- or in light-adapted conditions. The offset value was applied to the case of AR3 for comparison. The insert shows purified BcHeR in the buffer solution. (b) HPLC patterns of retinal oximes for AR3 and BcHeR in dark- and in light-adapted conditions. The symbols, 'Ts', 'Ta', '13s' and '13a', represent all-*trans*-15-*syn*, all-*trans*-15-*anti*, 13-*cis*-15-*syn* and 13-*cis*-15-*anti* retinal oxime, respectively (see Figure 4(a)). The compositions of each retinal isomer were calculated from the areas of the peaks (A_{Ts}, A_{Ta}, A_{13s}, and A_{13a}) in the HPLC patterns. For BcHeR, regardless of conditions, the ratio of the all-*trans* form to the 13-*cis* form, (A_{Ts} + A_{Ta}) / (A_{13s} + A_{13a}), was approximately 88 %. As a reference, for AR3 in dark-adapted condition, the normalized areas of peaks were 1.0 for A_{Ts}, 0.37 for A_{Ta}, 0.97 for A_{13s}, and 0.48 for A_{13a}, respectively.

chloride-pumping halorhodopsin[37] and sulfate (ion)-pumping rhodopsin.[38] Such spectral measurements may be a possible future work to identify clues to reveal the function of BcHeR.

The protonated Schiff base and its counterion generally play a key role for microbial rhodopsins in producing their functions[1,39,40] and the pK_a values for these residues could be function-determinant[30,41]. As seen in Figure 4(a) and the sequence alignment in Figure S2, the

retinal of BcHeR is predicted to be bound to a lysine residue (K253) in the seventh helix via a protonated Schiff base linkage, which would be electrically stabilized by a negatively charged residue as a counterion (presumably E118 for BcHeR). To estimate such pK_a values for a protonated Schiff base linkage with K253 and its counterion of BcHeR, we performed spectroscopic pH titration experiments. The purified BcHeR was suspended in a 6-mix buffer consisting of citric acid, MES, TES, TAPS, CHES and CAPS, a buffer that avoids drastic pH changes due to its buffer action over a wide pH range from 3 to 11. The pH-dependent spectral changes under acidic conditions are first shown in Figure 4(b). They exhibited a small spectral red-shift, which likely represents the protonation of the counterion and a corresponding decrease of the energy gap between the electronic ground and excited states. The difference spectra in Figure 4(c) show an absorbance increase at around 610 nm, which contributed to the spectral red-shift in Figure 4(b). Due to protein denaturation, the absorbance at 390 nm also increased as the pH values lowered and thus the pH-dependent spectral changes were irreversible. As well as for HeR-48C12, an absorbance increase in the UV region (around 400 nm) was observed, probably due to protein denaturation.[18] Therefore, heliorhodopsins may be intrinsically unstable under acidic conditions. Yet, for BcHeR, an isosbestic point at around 590 nm could still be seen and a significant denaturation as signified by the increasing absorption at around 390 nm was not observed below the pH of 4.5. Although a titration curve using the shift of absorption maxima against pH values in Figure 4(d) cannot estimate the correct pK_a of the counterion, the pK_a should be at least smaller than 4.5. This result clearly indicates that the counterion is deprotonated at neutral pH value.

A pH titration experiment under alkaline conditions was also performed to estimate the pK_a value of the protonated Schiff base (K253). Usually, deprotonation of the protonated Schiff base under alkaline conditions causes a large spectral blue-shift to the UV region (around 390 nm),[42] which appears clearly in Figures 4(e) and 4(f). However, protein denaturation under alkaline conditions also exhibits a spectral blue-shift similar to that caused by deprotonation of the protonated Schiff base, therefore requiring us to identify the cause for the spectral change in Figures 4(e) and 4(f). To clarify this point, we estimated how much protein denaturation occurs at each pH value as follows; the absorption spectrum A_b is measured at pH = 7, NaOH is added to the sample until the pH reaches the target value after which HCl is added to get the original pH of 7 again. The absorption spectrum A_a is measured and the difference in absorbance between those spectra ($\Delta A = A_b - A_a$) is considered as the amount of protein denaturation (data not shown). The data revealed that the spectral blue-shift comes mostly from protein denaturation and thus it can be concluded that deprotonation of the Schiff base was not observed at least over pH values from 7 to 11. Due to such protein instability under an alkaline pH, the exact pK_a value of the Schiff base (K253) could not be estimated. As shown in Figure 4(g), since the amount of protein

denaturation is small enough at pH values of less than 10, the pK_a of the Schiff base should be at least larger than 10, indicating that the Schiff base is protonated at a neutral pH value. As

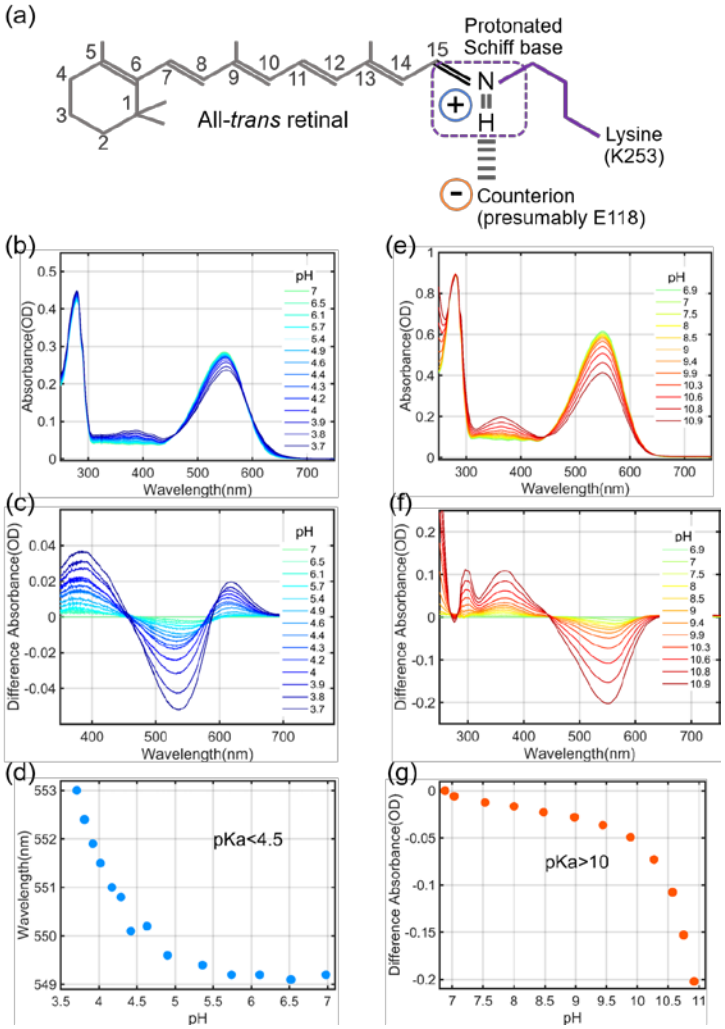

Figure 4. Absorption spectra of BcHeR at various pH values. The sample was suspended in a 6-mix buffer (0.89 mM citric acid, 0.89 mM MES, 1.1 mM TES, 0.78 mM TAPS, 1.1 mM CHES and 0.33 mM CAPS) with 300 mM NaCl and 0.05% DDM. The pH was adjusted to the desired value by adding concentrated HCl or NaOH. (a) Schematic of all-*trans* retinal bound to opsin with many carbon atoms in BcHeR. The retinal is specifically bound to a lysine residue (K253) through a protonated Schiff base that is electrically stabilized by a counterion (presumably E118). (b) Absorption and (c) difference absorption spectra at acidic pH values. The difference spectra were obtained with the spectrum at a pH of 7 as a baseline. (d) pH titration curve at acidic condition using the absorption maxima at around 550 nm. The absorption maxima were red-shifted as the pH values lowered, which is presumed to reflect the protonation of the counterion, E118. Considering that an isosbestic point at 590 nm was clearly seen and a significant denaturation as signified by the increasing absorption at around 390 nm was not observed below the pH of 4.5 in (c), the pK_a of the counterion E118 is presumed to be at least smaller than 4.5. (e) Absorption and (f) difference spectra at alkaline pH values. The difference spectra were obtained with the spectrum at a pH of 7 as a baseline. (g) pH titration curve at alkaline pH values using the difference absorbance at 550 nm. The pK_a of the Schiff base linked to K253 was not estimated because the absorbance decrease at 550 nm was irreversible mainly due to denaturation of the proteins. Since the protein denaturation is small enough at pH values of less than 10, the pK_a of the Schiff base should be larger than 10.

summarized in Table 1, both in BcHeR and in HeR-48C12, the Schiff base and the counterion are protonated and deprotonated at neutral pH values respectively, indicating the functional importance of the salt bridge between the Schiff base and the counterion.

Photocycle.

Illumination of short-pulsed light to microbial rhodopsins causes the photoisomerization from all-*trans* to 13-*cis* retinal, subsequently triggering a cyclic series of reactions called the 'photocycle' within millisecond to second time frames.[1,30] A typical photocycle contains various photo-intermediates, such as the K, M, and O intermediates, whose names and characteristics have been established for BR.[30] Most importantly, during the photocycle, there is an intermediate presenting the changes in the helical conformation and/or the ion-affinity that are required for functions such as ion transport and photo-sensory transduction. To observe such a photocycle for BcHeR, we performed time-resolved flash-photolysis measurements. Purified BcHeR was prepared in buffer at a pH of 7 in which the Schiff base and its counterion are protonated and deprotonated, respectively, according to the results shown in Figure 4. The sample was then excited with pulsed laser light and absorbance changes were recorded at each wavelength during the elapsed time *t* from 10 μs to 20 s.

Figure 5(a) shows the difference absorbance spectra at each elapsed time ranging from 380 nm to 720 nm. While many type-1 rhodopsins and heliorhodopsin HeR-48C12 show absorbance changes at around 400 nm, which reflect the presence of the M intermediate where the retinal-binding Schiff base is deprotonated,[18,30] BcHeR did not show such an absorbance change at 400 nm within the time-resolution of our measurements. This result raises two possibilities; one is that the rise and decay of the M intermediate is too fast to be detectable, while the other is the lack of an M intermediate as seen in anion-pump halorhodopsin.[43] On the other hand, the rise in absorbance at 625 nm and the synchronous decay at 525 nm are assignable to formation of the O intermediate where the retinal reisomerization to the all-*trans* form would take place. Figure 5(b) shows the time course of the difference absorbance at representative wavelengths (400 nm, 525 nm and 625 nm). The difference absorbance at 625 nm showed the presence of some intermediate even at the onset of the measurement (t = 10 μs), which is presumably the K-like intermediate representing an early photo-intermediate with the retinal isomerization. The absorbance at 625 nm then rose gradually in a sub-millisecond time scale, which can be interpreted as the formation of the O intermediate as mentioned above. This O intermediate continued to accumulate over around 100 ms and then slowly depleted within 10 s. The time course of the absorbance at 525 nm was synchronized but inverted in the amplitude compared with that at 625 nm. These curves were able to be fitted well with two exponential curves, meaning the formation and the depletion of the O intermediate. The time constants τ_1 and τ_2 were 0.6 ms and 1.7 s, respectively, and these were comparable to those observed in HeR-

48C12 (τ_1: 2 ms and τ_2: 0.8 s). If the M intermediate can be assumed to be present, an absorbance change at 400 nm should be observed between the K and the O intermediates. However, the measured absorbance change at 400 nm did not show any accumulation. It should be noted that HeR-48C12 contains two retinal isomers of 40 % all-*trans* and 60 % 13-*cis* forms in the light-adapted state, resulting in two independent reactions. In contrast, BcHeR predominantly contains all-*trans* retinal in both the dark- and the light-adapted states, providing only a single reaction. This difference between these heliorhodopsins might be the reason for the lack of an M intermediate in BcHeR.

Based on these results, we propose a photocycle model for BcHeR as shown schematically in Figure 5(c). After excitation with the light pulse at 550 nm, the retinal is immediately isomerized from the all-*trans* to the 13-*cis* form and the K intermediate at 625 nm is formed within 10 μs. Assuming that the M intermediate is present after the K intermediate, the protonated Schiff base and its counterion are expected be deprotonated and protonated at the M formation as seen in many type-1 rhodopsins.[1,30] Interestingly, however, the counterion E107 in HeR-48C12 proved not to act as a proton acceptor from the mutation analysis,[18] and thereby the counterion (presumably E118) in BcHeR is also unlikely to be a proton acceptor. After the K intermediate, the O intermediate is formed with the time constant τ_1 of 0.6 ms and continued to accumulate over 100 ms. In many microbial rhodopsins,[44] the retinal is reisomerized to the all-*trans* form upon formation of the O intermediate. Thus, the isomerized retinal for BcHeR is presumed to recover the all-*trans* configuration at the O intermediate. Considering such a characteristic long-life of the O intermediate compared with BR (Table 1), the O intermediate might be causing large conformational changes that correspond to an active state for some unidentified function in BcHeR. According to previous works for HeR-48C12,[18,27] one possible function is signal transduction since the long-lived O intermediate is a typical characteristic of sensory rhodopsin.[1] Another possible function is the transport of glycopeptides and/or amphiphilic molecules since BcHeR is derived from a gram-negative bacterium that would possess only an inner membrane. Finally, the O intermediate decays with a time constant τ_2 of 1.7 s and the original state is recovered within 10 s.

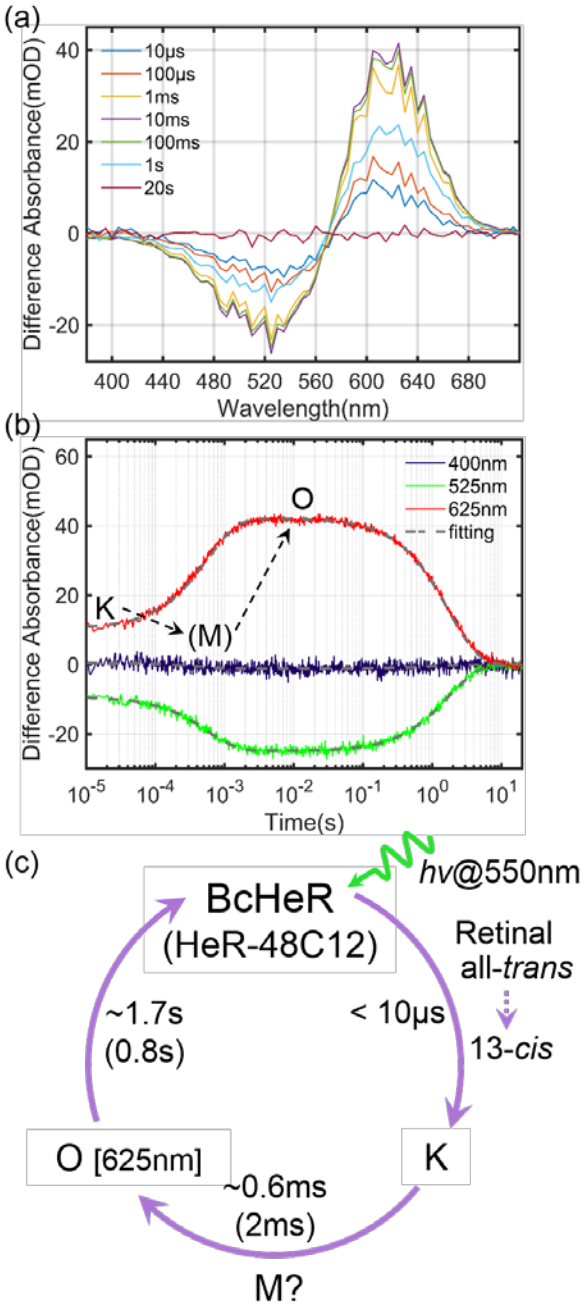

Figure 5. Time-resolved flash-photolysis with 550 nm pulsed light. (a) Transient absorption spectra ranging from a 10 μs to a 20 s time frame. (b) Time evolution of the absorption spectra at representative wavelengths of 400 nm (blue), 525 nm (green) and 625 nm (red). For the absorbance at 625 nm, the accumulation at the onset of the measurement (t = 10^{-5} s) represents the K intermediate and the subsequent increase represents the O intermediate. These three curves were fitted well using two exponential equations (dotted black lines). (c) Photocycle model. The flash light at 550 nm initiates the photocycle of BcHeR. During the transition from an original state to the K intermediate, the retinal is isomerized from the all-*trans* to the 13-*cis* form. The K intermediate then decays and the O intermediate emerges with a time constant τ_1 of 0.6 ms (2 ms for HeR-48C12). An M intermediate may exist between the K and O intermediates although it is not detectable in our experiment. At the end, the O intermediate decays and the original state recovers with a time constant τ_2 of 1.7 s (0.8 s for HeR-48C12). The isomerized retinal is presumed to return back to the all-*trans* form at the O intermediate.

Table 1. Summarized photochemical properties for BcHeR and HeR-48C12 from heliorhodopsins, and bacteriorhodopsin (BR) from type-1 rhodopsin.

Opsin	Fraction	λmax (nm)	All-*trans* in retinal configuration (%)	pKa value	Decay constant of O intermediate (s)
BcHeR	Gram-negative bacteria	550	Dark: 88% Light: 88%	Schiff base: >10 (K253) Counterion: <4.5 (E118)	~1.7
HeR-48C12	Gram-positive bacteria	551	Dark: 97%[18] Light: 40%[18]	Schiff base: 11.5 (K241)[18] Counterion: 3.7(E107)[18]	~0.8[18]
BR	Archaea	570	Dark: 50%[34] Light: 100%[34]	Schiff base: 13.3 (K216)[31] Counterion: 2.6 (D85)[31]	~0.002[30]

CONCLUSION

This study aimed to identify photochemical properties that are conserved and are not conserved between BcHeR from a gram-negative eubacterium and HeR-48C12 from a gram-positive eubacterium. As a property that is not conserved, the adaptation state of retinal to dark- or light-condition was absent in BcHeR based on HPLC patterns while HeR-48C12 shows the light-adaptation state. In contrast, conserved properties between BcHeR and HeR-48C12 were also identified: the ion-transport activity is not observed; the Schiff base and the counterion are respectively protonated and deprotonated at neutral pH; there exists the second-scale long-lived O intermediate during the photocycle which may activate their unidentified function. We believe that these findings provide a basis for understanding common characteristics of the heliorhodopsins.

As a future work, we will first perform extensive mutation analysis to experimentally identify the residues for Schiff base, the counterion and the proton acceptor of Schiff base in BcHeR. Next, we will measure dose-dependent maximum absorbance changes under different ions in the native organism expressing BcHeR for revealing the possible function of BcHeR. Through the further understanding of BcHeR from the above possible experiments, we would like to explore the nature of the heliorhodopsins.

Supporting Information

Amino acid alignment among the heliorhodopsin family, amino acid alignment of BcHeR, HeR-48C12 and various type-1 microbial rhodopsins, and lists of rhodopsins with accession numbers used in Figure 1(a).

Accession Codes

Hypothetical protein [*Bellilinea caldifistulae*] KPL76735.1

Heliorhodopsin 48C12 [Actinobacterium] AVZ43932

Corresponding Author

*Email: sudo@okayama-u.ac.jp.

ORCID

Yuki Sudo: 0000-0001-8155-9356

Acknowledgements

We thank Marie Kurihara and Akimasa Kaneko for technical supports in implementing the experiments. We also thank "DASS Manuscript" (http://www.dass-ms.com/home.html) for the English language review.

Funding

This work was financially supported by JSPS-KAKENHI Grant Number JP18H06051 to A.S., 18H04136 to S. Y., and JP15H04363, JP15H00878, JP25104005 and JP17H05726 to Y.S. This work was also supported by JST-CREST (JPMJCR1656) to Y.S., and AMED (17933570) to Y.S.

Notes

The authors declare no competing financial interests.

REFERENCES

(1) Hoff, W. D., Jung, K.-H., and Spudich, J. L. (1997) Molecular Mechanism of photosignaling by archaeal sensory rhodopsins. *Annu. Rev. Biophys. Biomol. Struct. 26*, 223–258.

(2) Oesterhelt, D., and Stoeckenius, W. (1971) Rhodopsin-like protein from the purple membrane of *Halobacterium halobium*. *Nat. New Biol. 233*, 149–152.

(3) Bamberg, E., Tittor, J., and Oesterhelt, D. (1993) Light-driven proton or chloride pumping by halorhodopsin. *Proc. Natl. Acad. Sci. 90*, 639–643.

(4) Béjà, O., Spudich, E. N., Spudich, J. L., Leclerc, M., and DeLong, E. F. (2001) Proteorhodopsin phototrophy in the ocean. *Nature 411*, 786–789.

(5) Inoue, K., Ono, H., Abe-Yoshizumi, R., Yoshizawa, S., Ito, H., Kogure, K., and Kandori, H. (2013) A light-driven sodium ion pump in marine bacteria. *Nat. Commun. 4*, 1678.

(6) Inoue, S., Yoshizawa, S., Nakajima, Y., Kojima, K., Tsukamoto, T., Kikukawa, T., and Sudo, Y. (2018) Spectroscopic characteristics of *Rubricoccus marinus* xenorhodopsin (RmXeR) and a putative model for its inward H^+ transport mechanism. *Phys. Chem. Chem. Phys. 20*, 3172–3183.

(7) Nagel, G., Ollig, D., Fuhrmann, M., Kateriya, S., Musti, A. M., Bamberg, E., and Hegemann, P. (2002) Channelrhodopsin-1: A light-gated proton channel in green algae. *Science 296*, 2395–2398.

(8) Govorunova, E. G., Sineshchekov, O. A., Janz, R., Liu, X., and Spudich, J. L. (2015) Natural light-gated anion channels: A family of microbial rhodopsins for advanced optogenetics. *Science 349*, 647–650.

(9) Spudich, J. L., and Bogomolni, R. A. (1984) Mechanism of colour discrimination by a bacterial sensory rhodopsin. *Nature 312*, 509–513.
(10) Takahashi, T., Tomioka, H., Kamo, N., and Kobatake, Y. (1985) A photosystem other than PS370 also mediates the negative phototaxis of *Halobacterium halobium*. *FEMS Microbiol. Lett. 28*, 161–164.
(11) Irieda, H., Morita, T., Maki, K., Homma, M., Aiba, H., and Sudo, Y. (2012) Photo-induced regulation of the chromatic adaptive gene expression by *Anabaena* sensory rhodopsin. *J. Biol. Chem. 287*, 32485–32493.
(12) Sineshchekov, O. A., Jung, K.-H., and Spudich, J. L. (2002) Two rhodopsins mediate phototaxis to low- and high-intensity light in *Chlamydomonas reinhardtii*. *Proc. Natl. Acad. Sci. 99*, 8689–8694.
(13) Fenno, L., Yizhar, O., and Deisseroth, K. (2011) The development and application of optogenetics. *Annu. Rev. Neurosci. 34*, 389–412.
(14) Ng, W. V., Kennedy, S. P., Mahairas, G. G., Berquist, B., Pan, M., Dutt Shukla, H., Lasky, S. R., Baliga, N. S., Thorsson, V., Sbrogna, J., Swartzell, S., Weir, D., Hall, J., Dahl, T. A., Welti, R., Goo, Y. A., Leithauser, B., Keller, K., Cruz, R., Danson, M. J., Hough, D. W., Maddocks, D. G., Jablonski, P. E., Krebs, M. P., Angevine, C. M., Dale, H., Isenbarger, T. A., Peck, R. F., Pohlschroder, M., Spudich, J. L., Jung, K.-H., Alam, M., Freitas, T., Hou, S., Daniels, C. J., Dennis, P. P., Omer, A. D., Ebhardt, H., Lowe, T. M., Liang, P., Riley, M., Hood, L., and Dassarma, S. (2000) Genome sequence of *Halobacterium* species NRC-1. *Proc. Natl. Acad. Sci. U. S. A. 97*, 12176–12181.
(15) Béjà, O., Aravind, L., Koonin, E. V., Suzuki, M. T., Hadd, A., Nguyen, L. P., Jovanovich, S. B., Gates, C. M., Feldman, R. A., Spudich, J. L., Spudich, E. N., and DeLong, E. F. (2000) Bacterial rhodopsin: Evidence for a new type of phototrophy in the sea. *Science 289*, 1902–1906.
(16) Martinez, A., Bradley, A. S., Waldbauer, J. R., Summons, R. E., and DeLong, E. F. (2007) Proteorhodopsin photosystem gene expression enables photophosphorylation in a heterologous host. *Proc. Natl. Acad. Sci. 104*, 5590–5595.
(17) Pushkarev, A., and Béjà, O. (2016) Functional metagenomic screen reveals new and diverse microbial rhodopsins. *ISME J. 10*, 2331–2335.
(18) Pushkarev, A., Inoue, K., Larom, S., Flores-uribe, J., Singh, M., Konno, M., Tomida, S., Nakamura, R., Tsunoda, P. S., Philosof, A., Sharon, I., Yutin, N., Eugene, V. K., Kandori, H., and Béjà, O. (2018) A distinct abundant group of microbial rhodopsins discovered using functional metagenomics. *Nature 558*, 595–599.
(19) Sudo, Y., Okazaki, A., Ono, H., Yagasaki, J., Sugo, S., Kamiya, M., Reissig, L., Inoue, K., Ihara, K., Kandori, H., Takagi, S., and Hayashi, S. (2013) A blue-shifted light-driven proton pump for neural silencing. *J. Biol. Chem. 288*, 20624–20632.

(20) Kumar, S., Stecher, G., Li, M., Knyaz, C., and Tamura, K. (2018) MEGA X: Molecular evolutionary genetics analysis across computing platforms. *Mol. Biol. Evol. 35*, 1547–1549.
(21) Edgar, R. C. (2004) MUSCLE: multiple sequence alignment with high accuracy and high throughput. *Nucleic Acids Res. 32*, 1792–1797.
(22) Jones, D. T., Taylor, W. R., and Thornton, J. M. (1992) The rapid generation of mutation data matrices from protein sequences. *CABIOS 8*, 275–282.
(23) Saitou, Naruya and Nei, M. (1987) The neighbor-Joining method: A new method for reconstructing phylogenetic trees. *Mol. Biol. Evol. 4*, 406–425.
(24) Sudo, Y., Ihara, K., Kobayashi, S., Suzuki, D., Irieda, H., Kikukawa, T., Kandori, H., and Homma, M. (2011) A microbial rhodopsin with a unique retinal composition shows both sensory rhodopsin II and bacteriorhodopsin-like properties. *J. Biol. Chem. 286*, 5967–5976.
(25) Yamada, T., Imachi, H., Ohashi, A., Harada, H., Hanada, S., Kamagata, Y., and Sekiguchi, Y. (2007) *Bellilinea caldifistulae* gen. nov., sp. nov and *Longilinea arvoryzae* gen. nov., sp. nov., strictly anaerobic, filamentous bacteria of the phylum *Chloroflexi* isolated from methanogenic propionate-degrading consortia. *Int. J. Syst. Evol. Microbiol. 57*, 2299–2306.
(26) Thiel, V., Hügler, M., Ward, D. M., and Bryant, D. A. (2017) The dark side of the mushroom spring microbial mat: Life in the shadow of chlorophototrophs. II. Metabolic functions of abundant community members predicted from metagenomic analyses. *Front. Microbiol. 8*, 943.
(27) Flores-Uribe, J., Hevroni, G., Ghai, R., Pushkarev, A., Inoue, K., Kandori, H., and Béjà, O. (2019) Heliorhodopsins are absent in diderm (Gram-negative) bacteria: some thoughts and possible implications for activity. *Environ. Microbiol. Rep. 11*, 419–424.
(28) Sutcliffe, I. C. (2011) Cell envelope architecture in the *Chloroflexi*: A shifting frontline in a phylogenetic turf war. *Environ. Microbiol. 13*, 279–282.
(29) Reynolds, S. M., Käll, L., Riffle, M. E., Bilmes, J. A., and Noble, W. S. (2008) Transmembrane topology and signal peptide prediction using dynamic bayesian networks. *PLoS Comput. Biol. 4*, e1000213.
(30) Lanyi, J. K. (2004) Bacteriorhodopsin. *Annu. Rev. Physiol. 66*, 665–688.
(31) Rousso, I., Friedman, N., Sheves, M., and Ottolenghi, M. (1995) pK_a of the protonated schiff base and aspartic 85 in the bacteriorhodopsin binding site is controlled by a specific geometry between the two residues. *Biochemistry 34*, 12059–12065.
(32) Inoue, K., Tsukamoto, T., Shimono, K., Suzuki, Y., Miyauchi, S., Hayashi, S., Kandori, H., and Sudo, Y. (2015) Converting a light-driven proton pump into a light-gated proton channel. *J. Am. Chem. Soc. 137*, 3291–3299.
(33) Chow, B. Y., Han, X., Dobry, A. S., Qian, X., Chuong, A. S., Li, M., Henninger, M. A., Belfort, G. M., Lin, Y., Monahan, P. E., and Boyden, E. S. (2010) High-performance genetically targetable optical neural silencing by light-driven proton pumps. *Nature 463*, 98–102.

(34) Otomo, A., Mizuno, M., Singh, M., Shihoya, W., Inoue, K., Nureki, O., Béjà, O., Kandori, H., and Mizutani, Y. (2018) Resonance raman investigation of the chromophore structure of heliorhodopsins. *J. Phys. Chem. Lett. 9*, 6431−6436.
(35) Pettei, M. J., Yudd, A. P., Nakanishi, K., Henselman, R., and Stoeckenius, W. (1977) Identification of retinal isomers isolated from bacteriorhodopsin. *Biochemistry 16*, 1955–1959.
(36) Vogeley, L., Sineshchekov, O. A., Trivedi, V. D., Sasaki, J., Spudich, J. L., and Luecke, H. (2004) *Anabaena* sensory rhodopsin: A photochromic color sensor at 2.0 Å. *Science 306*, 1390–1393.
(37) Varo, G., Needleman, R., and Lanyi, J. K. (1995) Light-driven chloride ion transport by Halorhodopsin from *Natronobacterium pharaonis*. 2. Chloride release and uptake, protein conformation change, and thermodynamics. *Biochemistry 34*, 14500–14507.
(38) Niho, A., Yoshizawa, S., Tsukamoto, T., Kurihara, M., Tahara, S., Nakajima, Y., Mizuno, M., Kuramochi, H., Tahara, T., Mizutani, Y., and Sudo, Y. (2017) Demonstration of a light-driven SO_4^{2-} transporter and its spectroscopic characteristics. *J. Am. Chem. Soc. 139*, 4376–4389.
(39) Sasaki, J., Brown, L. S., Chon, Y. S., Kandori, H., Maeda, A., Needleman, R., and Lanyi, J. K. (1995) Conversion of bacteriorhodopsin into a chloride ion pump. *Science 269*, 73–75.
(40) Marti, T., Khorana, H. G., Mogi, T., Stern, L. J., and Chao, B. H. (1988) Aspartic acid substitutions affect proton translocation by bacteriorhodopsin. *Proc. Natl. Acad. Sci. 85*, 4148–4152.
(41) Schweiger, U., Tittor, J., and Oesterhelt, D. (1994) Bacteriorhodopsin can function without a covalent linkage between retinal and protein. *Biochemistry 33*, 535–541.
(42) Kanehara, K., Yoshizawa, S., Tsukamoto, T., and Sudo, Y. (2017) A phylogenetically distinctive and extremely heat stable light-driven proton pump from the eubacterium *Rubrobacter xylanophilus* DSM 9941 T. *Sci. Rep. 4*, 44427.
(43) Váró, G. (2000) Analogies between halorhodopsin and bacteriorhodopsin. *Biochim. Biophys. Acta 1460*, 220–229.
(44) Ernst, O. P., Lodowski, D. T., Elstner, M., Hegemann, P., Brown, L. S., and Kandori, H. (2014) Microbial and animal rhodopsins: Structures, functions, and molecular mechanisms. *Chem. Rev. 114*, 126–163.